FEBS Letters 584 (2010) 2786–2790

FEBS Letters

journal homepage: www.FEBSLetters.org

Direct visualization of the small hydrophobic protein of human respiratory syncytial virus reveals the structural basis for membrane permeability

Stephen D. Carter, Kyle C. Dent, Elizabeth Atkins, Toshana L. Foster, Mark Verow, Petra Gorny, Mark Harris, Julian A. Hiscox, Neil A. Ranson, Stephen Griffin [1], John N. Barr *

Institute for Molecular and Cellular Biology, Faculty of Biological Sciences, University of Leeds, LS2 9JT, UK

ARTICLE INFO

Article history:
Received 14 April 2010
Revised 29 April 2010
Accepted 3 May 2010
Available online 20 May 2010

Edited by Jacomine Krijnse-Locker

Keywords:
Respiratory syncytial virus
Viroporin
Channel
SH protein

ABSTRACT

Human respiratory syncytial virus (HRSV) is the leading cause of lower respiratory tract disease in infants. The HRSV small hydrophobic (SH) protein plays an important role in HRSV pathogenesis, although its mode of action is unclear. Analysis of the ability of SH protein to induce membrane permeability and form homo-oligomers suggests it acts as a viroporin. For the first time, we directly observed functional SH protein using electron microscopy, which revealed SH forms multimeric ring-like objects with a prominent central stained region. Based on current and existing functional data, we propose this region represents the channel that mediates membrane permeability.

Structured summary:
MINT-7890792, MINT-7890805: *SH* (uniprotkb:P04852) and *SH* (uniprotkb:P04852) *bind* (MI:0407) by *chromatography technology* (MI:0091)
MINT-7890784, MINT-7890776: *SH* (uniprotkb:P04852) and *SH* (uniprotkb:P04852) *bind* (MI:0407) by *electron microscopy* (MI:0040)

1. Introduction

Human respiratory syncytial virus (HRSV) is the leading cause of lower respiratory tract disease in both infants and children, and as a consequence, the HRSV life-cycle, pathogenesis and interaction with the host cell are the subject of considerable research activity [1]. HRSV is classified within the *Paramyxoviridae* family of negative stranded RNA viruses, and expresses 11 known proteins from 10 genes. One of these is the small hydrophobic (SH) protein, which is 64 residues long with a hydrophobic core potentially comprising a single trans-membrane domain (Fig. 1A). The role of the SH protein in the HRSV life-cycle is unclear: It is non-essential for replication in cell culture, although SH-deleted HRSV replicated to 10-fold reduced titres in small animal models [2,3]. Furthermore, in chimpanzees, SH-deleted HRSV replicated to 40-fold lower titres than wild-type and exhibited considerably reduced rhinorrhea [4]. These studies show the SH protein is a virulence factor, playing a host-specific role in virus growth and pathology. Within infected cells, SH is present as an unmodified 7.5 kDa species, and as forms modified by carbohydrate addition, all of which oligomerize *in vivo*, and *in vitro* evidence suggest it exists predominantly as a pentamer [5,6]. Molecular modeling studies also favored the pentamer, and suggested SH adopts a circular structure with a central pore [7].

Several studies have indicated SH affects membrane permeability: Insertion into bacterial membranes resulted in increased entry of small molecules into cells [8], and when reconstituted in artificial membranes, peptides representing the trans-membrane domain displayed properties of a cation-selective ion channel [6]. These findings suggested SH may share features with small hydrophobic proteins of other RNA viruses, such as M2 of influenza A virus (IAV), p7 of hepatitis C virus (HCV), and 2B of poliovirus, all of which are categorized as viroporins [9]. These proteins are small, hydrophobic, able to homo-oligomerize, and induce membrane permeability to ions or small molecules, with diverse roles including virus assembly, entry, and manipulation of cellular ion homeostasis.

We generated full-length recombinant SH protein that was functional as a viroporin, and for the first time we visualized SH in a membrane-mimetic environment, which revealed SH formed ring-like multimers with a central cavity that we propose represents a channel.

2. Materials and methods

2.1. Plasmid construction

The SH cDNA was amplified from HRSV A2 infected cell RNA using primers designed to fuse the FLAG epitope (DYKDDDDK) to

* Corresponding author.
E-mail address: j.n.barr@leeds.ac.uk (J.N. Barr).
[1] Present address: Leeds Institute of Molecular Medicine, Wellcome Trust Brenner Building, St. James's University Hospital, University of Leeds, LS9 7TF, UK.

0014-5793 © 2010 Federation of European Biochemical Societies. Published by Elsevier B.V. Open access under CC BY-NC-ND license.
doi:10.1016/j.febslet.2010.05.006

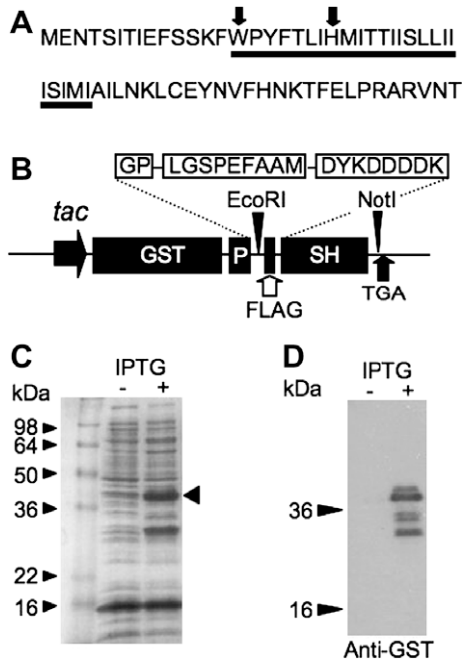

Fig. 1. (A) The SH protein sequence, with predicted trans-membrane domain underlined, and tryptophan and histidine residues marked. (B) pGEX-FLAG-SH, designed to express SH protein N-terminally fused to GST and FLAG, and containing a 3C cleavage site (P). Additional residues fused to the SH ORF are shown boxed. (C) PAGE analysis of expressed SH fusion protein from IPTG-induced or un-induced cultures. (D) Western blotting of IPTG-induced, or un-induced lysates using anti-GST antibody.

its N-terminus. FLAG-SH cDNA was inserted into pGEX-6P-1 (Amersham Biosciences) downstream of the glutathione-S-transferase (GST) ORF and the rhinovirus 3C protease site to yield pGST-FLAG-SH (Fig. 1B). The FLAG-SH protein was predicted to be 86 residues long, with a mass of 9890 Da, including additional N-terminal residues (GP) remaining after protease cleavage, and plasmid-encoded residues at both N-(LGSPEFAAM) and C-termini (AAAS).

2.2. Expression and purification of GST-FLAG-SH

Inclusion body preparations containing insoluble GST-FLAG-SH were generated from IPTG-induced *Escherichia coli* BL21 cultures transformed with pGST-FLAG-SH, as previously described for HCV p7 [10]. GST was cleaved from FLAG-SH using Pre-Scission protease (Amersham Biosciences), and the resulting FLAG-SH protein was solubilized in 0.5% w/v N-laurylsarcosine (Sigma-Aldrich). HPLC was performed using a Dionex system using a C8 column eluted by a continuous 0–100% gradient of 80% v/v acetonitrile, 0.1% v/v trifluoroacetic acid. Collected fractions were lyophilized, and re-suspended in 100% methanol, or SDS–PAGE sample buffer.

2.3. PAGE and Western blotting

Fractions were analyzed using SDS–PAGE and visualized using Coomassie or silver staining, or were Western-blotted and identified using anti-GST (Sigma–Aldrich) or anti-FLAG M2 (Serotech) monoclonal antibodies, secondary horseradish peroxidase-linked antibody (Sigma–Aldrich), and in-house chemi-luminescence reagent.

2.4. Liposome preparation

Liposomes comprising phosphatidic acid, phospatidylcholine, and phosphatidylethanolamine with lisamine rhodamine-B labeled head groups (Avanti polar lipids) containing 50 mM carboxy-fluorescein (CF) (Sigma–Aldrich) were prepared by extrusion as described previously [11].

2.5. Viroporin assay

Dye-release was measured in real-time by fluorescence as previously described [11]. Briefly, assays were performed in 100 μl volumes, comprising 50 μM liposomes and various concentrations of FLAG-SH/methanol in HEPES-buffered saline (HBS; 10 mM HEPES-NaOH pH 7.4, 107 mM NaCl). Dye-release was measured using a FLUOstar Optima plate-reader (BMG Labtech) with excitation and emission wavelengths of 485 nm and 520 nm, respectively. Fluorescence was measured in triplicate at 30 s intervals, with experiments repeated twice. Melittin bee venom peptide (Sigma–Aldrich) was used as a positive control [12], and 0.1% (w/v) Triton X-100 to indicate maximal dye-release. Negative controls consisted of liposomes alone, or with methanol (5% and 10% final concentration), in the absence of SH protein.

2.6. Electron microscopy

Purified SH-FLAG fusion protein was applied to copper grids in PBS/1,2-diheptanoyl-sn-glycero-3-phosphocholine (DHPC), or in liposomes. Samples were blotted, negatively stained using 3% ammonium molybdate, and examined using a Tecnai F20 at a magnification of 62 000. Images were aligned and classified to generate groups of equivalently orientated projections. Separate class-averages were generated using SPIDER and IMAGIC programs [13,14].

2.7. Mass spectrometry

Lyophilized FLAG-SH was re-suspended in methanol/water (1:1), and samples were analyzed by Z-spray nanoelectrospray ionisation orthogonal time-of-flight MS on a Synapt HDMS device (Waters, UK). Data acquisition and processing was performed using MassLynx v4.1 software, and m/z spectra were transformed using MaxEnt.

2.8. Molecular modeling

SH protein secondary structure was predicted using MEMSAT3 and PSIPRED [15] and monomer models built using Maestro (Schrodinger). Models were energy minimized with residues 15-38 defined as the trans-membrane domain. Multiple monomers were aligned, with clusters of polar trans-membrane residues facing the pore lumen, and rearranged to regain symmetry and energy minimized as before.

3. Results

3.1. SH protein expression

Based on our previous experience with the HCV p7 viroporin [10], we expressed SH as a fusion protein linked at its N-terminus to GST and FLAG, with an intervening cleavage site for subsequent GST removal. The SH fusion protein was expressed in *E. coli* BL21 cells transformed with plasmid pGEX-FLAG-SH (Fig. 1B). Comparison of IPTG-induced and non-induced cultures identified a 40 kDa species (Fig. 1C), confirmed as the GST-FLAG-SH fusion protein by Western blotting using anti-GST antibody (Fig. 1D).

3.2. SH protein purification

Our previous work [10] showed that GST-FLAG-P7 accumulated within inclusion bodies that could be selectively harvested, and we

applied this approach to purify GST-FLAG-SH. Inclusion bodies containing GST-FLAG-SH were re-suspended and GST removed by cleavage, after which FLAG-SH protein was purified by HPLC (Fig. 2A). Peak fractions were pooled and subjected to PAGE analysis and Western blotting, which revealed the presence of discrete species having molecular weights ranging from 10 kDa to approximately 60 kDa (Fig. 2B and C). Interestingly, these species increased in 10 kDa increments, suggesting they represented FLAG-SH oligomers, in agreement with previous studies that showed SH readily multimerized. Interestingly, both silver staining and Western blotting detected low levels of monomeric FLAG-SH. One explanation was that FLAG-SH readily formed multimers that were resistant to denaturation, and similar findings have been reported for HCV p7 [16].

To further assess the purity of FLAG-SH, pooled peak fractions were analyzed by mass spectrometry, which identified one major species with a mass of 9892 Da, closely corresponding to the predicted mass of 9890 Da (Fig. 2D). This analysis confirms four important features of purified FLAG-SH protein: First, the purified protein was the correctly-cleaved FLAG-SH. Second, the high molecular weight species visualized by PAGE were FLAG-SH multimers. Third, FLAG did not affect SH multimerization, and fourth, FLAG-SH protein was highly pure.

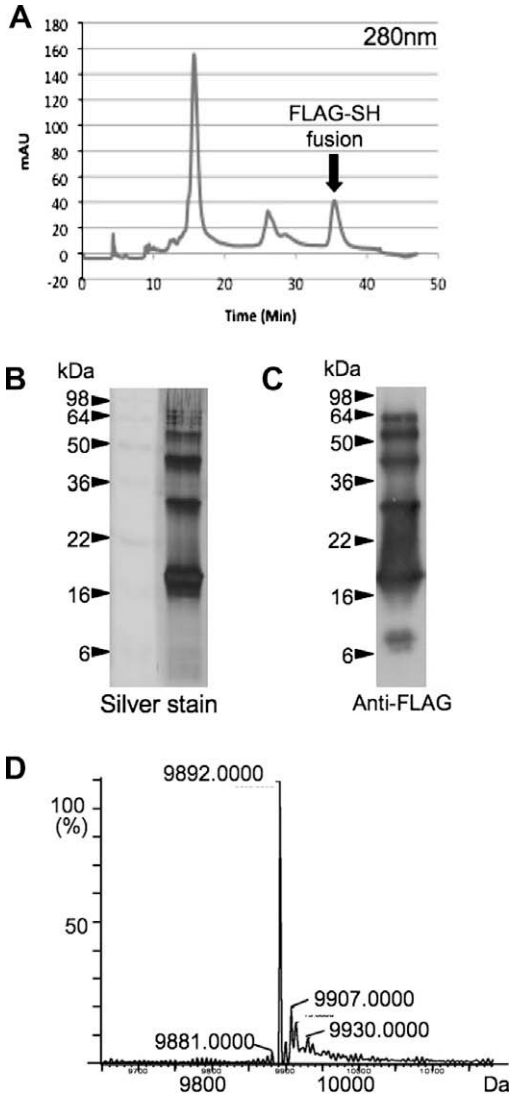

Fig. 2. (A) HPLC elution profile of FLAG-SH. Peak fractions were pooled and subjected to SDS-PAGE, and proteins visualized using (B) silver staining or (C) Western blotting using anti-FLAG antibody. (D) Mass spectrometry of FLAG-SH identified a peak at 9892 Da, which closely-matched the predicted mass (9890 Da).

3.3. Viroporin activity of FLAG-SH multimers

To test whether full-length recombinant FLAG-SH was functional, we tested its ability to induce membrane permeability using a previously described liposome dye-release assay [11]. This assay involved inserting the viroporin into liposomes filled with self-quenching concentrations of CF. Viroporin activity caused dye-release, and reduction of CF concentration caused fluorescence gain detected using fluorimetry. As a positive control to confirm assay function, liposomes were also incubated with melittin bee venom peptide, which forms a membrane pore that mediates high-level dye-release [11,12]. Base-line levels of fluorescence were calculated using solvent-only, and liposome-only controls.

Addition of FLAG-SH to the liposome preparation resulted in rapid dye-release, as measured by increasing fluorescence over base-line levels, and when increasing quantities of purified protein were added, dye-release increased in a dose-dependant manner, suggesting FLAG-SH protein specifically mediated this effect, and thus was active as a viroporin (Fig. 3).

3.4. Direct visualization of SH oligomers

The above results showed FLAG-SH formed higher-order oligomers, which is reminiscent of other viroporins such as p7. Direct visualization of p7 using EM showed it formed hexameric or heptameric ring-like structures with diameters of 8.1 nm [16], or 10 nm [10]. These structures displayed central features thought to represent channels, and the current model for p7 activity suggests this channel provides the structural basis for membrane permeability by allowing passage of ions and small molecules. Because SH shares many biochemical properties with p7, we hypothesized that SH viroporin activity may also depend on a central pore.

To test this hypothesis, we directly visualized functionally active SH multimers using EM. HPLC purified FLAG-SH was mixed with either liposomes or the membrane-mimetic detergent DHPC, which induces multimerization of both HCV p7 and IAV M2 [11,16,17], applied to carbon grids and negatively stained. Direct observation identified abundant structures of ring-like morphology, which could be predominantly categorized into two groups having discrete diameters of 8.7 nm or 9.3 nm (Fig. 4A). Both larger and smaller structures were also observed, but with considerably

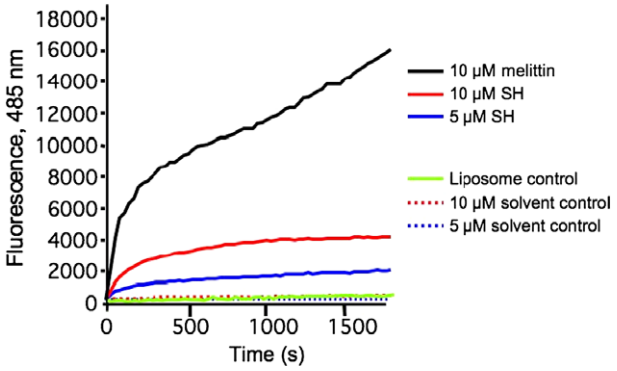

Fig. 3. FLAG-SH was incorporated into liposomes, and CF dye-release monitored by fluorimetry. Mean values of 6 experiments show SH-mediated dye release above the corresponding solvent-only and liposome-only controls. Methanol and liposome only values are also shown for completeness. The membrane channel melittin was incorporated into liposomes as a positive control.

lower abundance. All ring-like objects possessed a darkly stained central region that could represent a pore or channel. In addition, smaller structures without ring morphology were observed that likely represented side views.

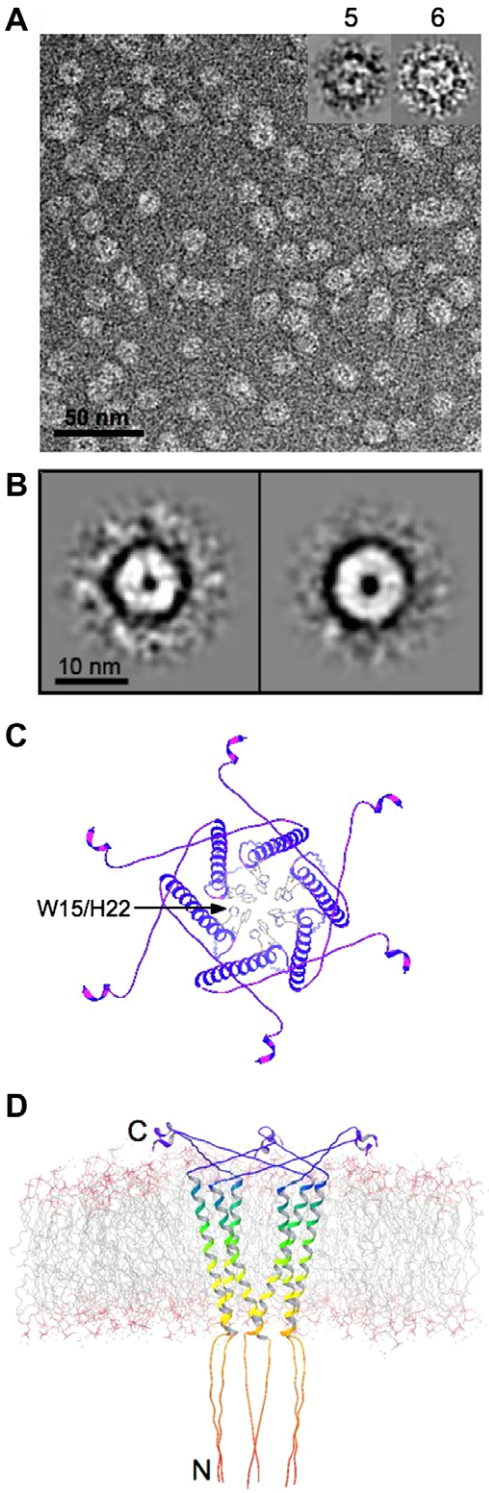

Fig. 4. (A) Direct EM observation of FLAG-SH using negative staining, with individual representatives of putative pentamer (5) and hexamer (6) classes shown at higher magnification. (B) Putative pentamer and hexamer class-averages. (C) Molecular model of full-length SH protein as a hexamer. W15/H22 residues within the trans-membrane domain are shown within the putative channel lumen. (D) Model of the SH hexamer inserted into a PAPC bilayer, as used in the liposome assay.

Following image processing to generate class-averages, the 8.7 and 9.3 nm structures displayed distinctive 5-fold and 6-fold symmetry, respectively, strongly suggesting they corresponded to pentamers and hexamers (Fig. 4B), consistent with our PAGE analysis (Fig. 2B). Class averages revealed increased definition of the central pore, which displayed diameters of 1.9 and 2.6 nm for the putative pentamer and hexamer forms, respectively. In addition, the unstained protein component of these rings was unchanged in width. Taken together, these observations are consistent with assembly of a ring from monomeric units of constant dimensions forming a central void visible with negative staining, such that when monomers were added, the width of the protein ring did not change, but the pore diameter increased correspondingly.

This represents the first direct confirmation that full-length, functional SH protein is capable of oligomerizing in membrane-mimetic environments forming a channel-like structure, and further confirms that SH belongs to the viroporin family of ion channels.

4. Discussion

Despite the importance of SH protein in the HRSV life cycle, the mechanism by which it contributes to virulence remain unclear. Several independent lines of evidence indicate SH induces membrane-permeability, and two models have previously been discussed describing how the poliovirus 2B viroporin may perform this activity [18]: The first posits that amphipathic helices form membrane-spanning oligomers, with hydrophobic residues facing the membrane and hydrophilic side-groups forming a pore through which ions and small molecules pass. This model suggests such assemblies are restricted to defined oligomeric states, depending on structural characteristics of component monomers. The second model postulates that viroporin amphipathic helices lie parallel to the membrane surface, forming a "carpet-like" structure that induces permeability by disrupting membrane architecture. This model predicts dimensions and multimer composition of these assemblies would be indeterminate.

To distinguish between these possibilities, and advance our understanding of the SH structure-function relationship, we performed direct EM observation and single-particle averaging of functional viroporin structures. This analysis revealed ring-like objects that predominantly exhibited 5-fold and 6-fold symmetry, which likely represented pentamers and hexamers, all containing a central pore. These observations are only consistent with the first model described above.

We measured the central pore at 1.9 nm for the pentamer and 2.6 nm for the hexamer. Pores of these dimensions would allow passage of not only ions, but also small molecules, and this is entirely consistent with experimental observations that show SH induces membrane permeability to both hygomycin [8] and CF. In contrast, the previous model [7] derived from molecular dynamics simulations predicted a pore diameter of 0.15 nm, which is inconsistent with either our experimental EM observations, or current and previous functional assays.

Based on our results, we present an updated hexamer model (Fig. 4C and D). In advance of structural analysis by three-dimensional reconstruction, NMR and crystallography, this model reveals possible three-dimensional arrangement of residues, and will guide mutagenesis to further explore the SH structure/function relationship. Interestingly, this model predicts conserved tryptophan-15 is positioned at the channel entrance, which has been suggested [6] to be analogous to tryptophan-41 that lines the IAV M2 channel lumen, and gates ion-channel function [17]. M2 gate movement is triggered by protonation of histidine-37, and similar relative positioning of tryptophan and histidine residues is conserved in HCV p7. Interestingly, the HRSV SH protein also possesses

a single histidine residue proximal to tryptophan-15, which could perform the same role (Figs. 1A and 4C). The putative model also suggests that positively charged residues R59 and R61 within the short C-terminal helix may stabilize the assembly by interacting with the membrane surface.

More recently, the HRSV SH protein has been suggested to possess anti-apoptosis activity [19]. How this function correlates with viroporin activity is unclear. However, as changes in membrane permeability are features of apoptotic pathways, it is interesting to speculate that HRSV SH may counteract apoptosis by reversing specific permeability changes. Furthermore, as other paramyxoviruses such as parainfluenza virus-5 and mumps virus also express structurally similar SH proteins, with similarly reported anti-apoptotic activities, it will be interesting to investigate whether they also form viroporins.

Acknowledgements

K.D. and T.F. are supported by Wellcome Trust studentships. E.A. is supported by a BBSRC/Pfizer CASE studentship. J.N.B. is an RCUK fellow and S.G. is recipient of a University of Leeds Biomedical Health Research Centre senior translational research fellowship. HPLC was performed in the Wellcome Trust-funded centre for biomolecular interactions.

References

[1] Collins, P.L. and Graham, B.S. (2008) Viral and host factors in human respiratory syncytial virus pathogenesis. J. Virol. 82, 2040–2055.
[2] Bukreyev, A., Whitehead, S.S., Murphy, B.R. and Collins, P.L. (1997) Recombinant respiratory syncytial virus from which the entire SH gene has been deleted grows efficiently in cell culture and exhibits site-specific attenuation in the respiratory tract of the mouse. J. Virol. 71, 8973–8982.
[3] Jin, H., Zhou, H., Cheng, X., Tang, R., Munoz, M. and Nguyen, N. (2000) Recombinant respiratory syncytial viruses with deletions in the NS1, NS2, SH, and M2-2 genes are attenuated in vitro and in vivo. Virology 273, 210–218.
[4] Whitehead, S.S., Bukreyev, A., Teng, M.N., Firestone, C.Y., St Claire, M., Elkins, W.R., Collins, P.L. and Murphy, B.R. (1999) Recombinant respiratory syncytial virus bearing a deletion of either the NS2 or SH gene is attenuated in chimpanzees. J. Virol. 73, 3438–3442.
[5] Collins, P.L. and Mottet, G. (1993) Membrane orientation and oligomerization of the small hydrophobic protein of human respiratory syncytial virus. J. Gen. Virol. 74 (Pt 7), 1445–1450.
[6] Gan, S.W., Ng, L., Lin, X., Gong, X. and Torres, J. (2008) Structure and ion channel activity of the human respiratory syncytial virus (hRSV) small hydrophobic protein transmembrane domain. Protein Sci. 17, 813–820.
[7] Kochva, U., Leonov, H. and Arkin, I.T. (2003) Modeling the structure of the respiratory syncytial virus small hydrophobic protein by silent-mutation analysis of global searching molecular dynamics. Protein Sci. 12, 2668–2674.
[8] Perez, M., Garcia-Barreno, B., Melero, J.A., Carrasco, L. and Guinea, R. (1997) Membrane permeability changes induced in *Escherichia coli* by the SH protein of human respiratory syncytial virus. Virology 235, 342–351.
[9] Gonzalez, M.E. and Carrasco, L. (2003) Viroporins. FEBS Lett. 552, 28–34.
[10] Clarke, D., Griffin, S., Beales, L., Gelais, C.S., Burgess, S., Harris, M. and Rowlands, D. (2006) Evidence for the formation of a heptameric ion channel complex by the hepatitis C virus p7 protein in vitro. J. Biol. Chem. 281, 37057–37068.
[11] StGelais, C., Tuthill, T.J., Clarke, D.S., Rowlands, D.J., Harris, M. and Griffin, S. (2007) Inhibition of hepatitis C virus p7 membrane channels in a liposome-based assay system. Antiviral Res. 76, 48–58.
[12] Schwarz, G., Zong, R.T. and Popescu, T. (1992) Kinetics of melittin induced pore formation in the membrane of lipid vesicles. Biochim. Biophys. Acta 1110, 97–104.
[13] Shaikh, T.R., Gao, H., Baxter, W.T., Asturias, F.J., Boisset, N., Leith, A. and Frank, J. (2008) SPIDER image processing for single-particle reconstruction of biological macromolecules from electron micrographs. Nat. Protoc. 3, 1941–1974.
[14] van Heel, M., Harauz, G., Orlova, E.V., Schmidt, R. and Schatz, M. (1996) A new generation of the IMAGIC image processing system. J. Struct. Biol. 116, 17–24.
[15] Jones, D.T. (2007) Improving the accuracy of transmembrane protein topology prediction using evolutionary information. Bioinformatics 23, 538–544.
[16] Luik, P. et al. (2009) The 3-dimensional structure of a hepatitis C virus p7 ion channel by electron microscopy. Proc. Natl. Acad. Sci. U.S.A. 106, 12712–12716.
[17] Schnell, J.R. and Chou, J.J. (2008) Structure and mechanism of the M2 proton channel of influenza A virus. Nature 451, 591–595.
[18] Agirre, A., Barco, A., Carrasco, L. and Nieva, J.L. (2002) Viroporin-mediated membrane permeabilization. Pore formation by nonstructural poliovirus 2B protein. J. Biol. Chem. 277, 40434–40441.
[19] Fuentes, S., Tran, K.C., Luthra, P., Teng, M.N. and He, B. (2007) Function of the respiratory syncytial virus small hydrophobic protein. J. Virol. 81, 8361–8366.